

Nucleon- α scattering and resonances in ^5He and ^5Li with JISP16 and Daejeon16 NN interactions

A. M. Shirokov,^{1,2,3} A. I. Mazur,³ I. A. Mazur,³ E. A. Mazur,³ I. J. Shin,⁴ Y. Kim,⁴ L. D. Blokhintsev,^{1,3} and J. P. Vary²

¹*Skobeltsyn Institute of Nuclear Physics, Lomonosov Moscow State University, Moscow 119991, Russia*

²*Department of Physics and Astronomy, Iowa State University, Ames, Iowa 50011, USA*

³*Department of Physics, Pacific National University, Khabarovsk 680035, Russia*

⁴*Rare Isotope Science Project, Institute for Basic Science, Daejeon 305-811, Korea*



(Received 13 August 2018; published 29 October 2018)

The approach called the single-state harmonic oscillator representation of scattering equations (SS-HORSE) to analyze resonant states is generalized to the case of charged particle scattering by using the analytical properties of partial scattering amplitudes and is applied to the study of resonant states in the ^5Li nucleus and nonresonant s -wave proton- α scattering within the no-core shell model using the JISP16 and Daejeon16 NN interactions. We present also the results of calculations of neutron- α scattering and resonances in the ^5He nucleus with Daejeon16 and compare with results published previously using JISP16.

DOI: [10.1103/PhysRevC.98.044624](https://doi.org/10.1103/PhysRevC.98.044624)

I. INTRODUCTION

There is considerable progress in developing *ab initio* methods for studying nuclear structure [1] based on a rapid development of supercomputer facilities and recent advances in the utilization of high-performance computing systems. In particular, modern *ab initio* approaches, such as the Green's function Monte Carlo (GFMC) [2], the hyperspherical expansion [1], the no-core shell model (NCSM) [3], the coupled-cluster theory [4,5], and the nuclear lattice effective field theory [6,7] are able to reproduce properties of atomic nuclei with mass up to $A = 16$ and selected heavier nuclear systems around closed shells.

Within the NCSM as well as within other variational approaches utilizing the harmonic-oscillator basis, the calculation of nuclear ground states and other bound states starts conventionally from estimating the dependence of the energy $E_\nu(\hbar\Omega)$ of the bound state ν in some model space on the harmonic-oscillator frequency $\hbar\Omega$. The minimum of $E_\nu(\hbar\Omega)$ is correlated with the energy of the state ν . The convergence of calculations and the accuracy of the energy prediction is estimated by comparing with the results obtained in neighboring model spaces. To improve the accuracy of theoretical predictions, various extrapolation techniques have been suggested recently [8–21] which make it possible to estimate the binding energies in the complete infinite basis space. The studies of extrapolations to the infinite model spaces reveal general trends of convergence patterns of variational calculations with the harmonic-oscillator basis, in the shell-model calculations in particular.

An extension of the *ab initio* methods to the studies of the continuum spectrum and nuclear reactions is one of the main-streams of modern nuclear theory. A remarkable success in developing the *ab initio* reaction theory was achieved in few-body physics where exact Faddeev and Faddeev–Yakubovsky equations [22] or the Alt, Grassberger, and Sandhas (AGS) method [23] are nowadays routinely used for calculating various few-body reactions.

The most important breakthrough in developing the *ab initio* theory of nuclear reactions in systems with total number of nucleons $A > 4$ was achieved by combining the NCSM and the resonating group method (RGM); the resulting approaches are conventionally referred to as NCSM/RGM and the no-core shell model with continuum (NCSMC) [3,24–26]. It is also worth noting the Lorentz integral transform approach to nuclear reactions with electromagnetic probes [1,27] and the GFMC calculations of elastic $n\alpha$ scattering [28]. Nuclear resonances can be also studied within the no-core Gamow shell model (NCGSM) [29].

Both NCGSM and NCSM/RGM complicate essentially the shell model calculations. A conventional belief is that the energies of shell model states in the continuum should be associated with the resonance energies. It was shown, however, in Refs. [30,31], that the energies of shell-model states may appear well above the energies of resonant states, especially for broad resonances. Moreover, the analysis of Refs. [30,31] clearly demonstrated that the shell model should also generate some states in a nonresonant nuclear continuum. In Refs. [32–36] we suggested an approach called the single-state harmonic oscillator representation of scattering equations (SS-HORSE), which provides an interpretation of the shell-model states in the continuum and makes it possible to deduce resonance energies and widths or low-energy nonresonant phase shifts directly from shell-model results without introducing additional Berggren basis states as in NCGSM or additional calculations as in the NCSM/RGM and NCSMC approaches.

The SS-HORSE approach is based on a simple analysis of the $\hbar\Omega$ and basis-size dependencies of the results of standard variational shell-model calculations. We have successfully applied it to extracting resonance energies and widths in $n\alpha$ scattering as well as nonresonant $n\alpha$ elastic-scattering phase shifts [32,33] from the NCSM calculations of ^5He and ^4He nuclei with the JISP16 NN interaction [37]. To describe democratic decays [38,39] of few-nucleon systems,

we developed a hyperspherical extension of the SS-HORSE method [40,41]. An application of this extended SS-HORSE approach to the study of the four-neutron system (tetra-neutron) [40–42] predicted for the first time a low-energy tetra-neutron resonance consistent with a recent experiment [43] with soft realistic NN interactions such as JISP16 [37], Daejeon16 [44], and similarity-renormalization-group-softened (SRG-softened) chiral effective field theory (χ EFT) NN interaction of Ref. [45].

In this contribution, we discuss an extension of the SS-HORSE method to the case of charged particle scattering. The SS-HORSE technique provides the S matrix or scattering phase shifts in some energy interval above the threshold where the shell-model calculations generate eigenstates with various $\hbar\Omega$ values and various basis truncations. Next we parametrize the S matrix to obtain it in a wider energy interval and to locate its poles associated with resonances. We have shown [32,33] that this parametrization should provide a correct description of low-energy phase shifts. The phase-shift parametrization utilized in Refs. [32–34] was derived from the symmetry properties of the S matrix. However, due to the long-range Coulomb interaction in the case of charged particle scattering, the analytical properties of the S matrix become much more complicated and cannot be used for its low-energy parametrization. In Ref. [35] we suggested a version of the SS-HORSE approach which utilizes the phase-shift parametrization based on analytical properties of the partial-wave scattering amplitude. In the case of charged particle scattering, instead of the partial-wave scattering amplitude, one can use the so-called renormalized Coulomb-nuclear amplitude [46,47] which has similar analytical properties. This opens a route to the generalization of the SS-HORSE method to the case of the charged particle scattering proposed in Ref. [36] where we have verified this approach by using a model problem of scattering of particles interacting by the Coulomb and a short-range potential. To calculate the Coulomb-nuclear phase shifts, we make use of the version of the HORSE formalism suggested in Ref. [48] and utilized later in our studies [30,31].

In this contribution we present the results of SS-HORSE calculations of proton- α resonant and nonresonant scattering phase shifts based on the *ab initio* NCSM results for ^5Li and ^4He nuclei obtained with the JISP16 [37] and a newer Daejeon16 [44] NN interactions derived from a χ EFT internucleon potential and better fitted to the description of light nuclei than JISP16. We search for the S -matrix poles to evaluate the energies and widths of resonant states in the ^5Li nucleus. The NCSM-SS-HORSE calculations of the ^5He resonant states have been performed with the JISP16 interaction in Refs. [32,33]. We present here also the results of the NCSM-SS-HORSE ^5He resonant state calculations with Daejeon16 to complete the studies of the nucleon- α resonances with the realistic JISP16 and Daejeon16 NN potentials. The previous *ab initio* analyses of nucleon- α resonances with various modern realistic internucleon interactions were performed in Ref. [28] within the GFMC, within the NCGSM in Ref. [29], within the coupled-cluster theory with Berggren basis in Ref. [49], and in Refs. [24,50–52] within the NCSM/RGM. We

note also a recent paper of Lazauskas [53] where the $n\alpha$ scattering was studied within a five-body Faddeev–Yakubovsky approach.

II. SS-HORSE METHOD FOR CHANNELS WITH NEUTRAL AND CHARGED PARTICLES

A. General formulas

The SS-HORSE approach relies on the J -matrix formalism in quantum scattering theory.

Originally, the J -matrix formalism was developed in atomic physics [54]; therefore, the so-called Laguerre basis was naturally used within this approach. A generalization of this formalism utilizing either the Laguerre or the harmonic oscillator bases was suggested in Ref. [55]. Later the harmonic-oscillator version of the J -matrix method was independently rediscovered by the Kiev (Filippov and collaborators) [56] and Moscow (Smirnov and collaborators) [57] groups. The J matrix with oscillator basis is sometimes also referred to as an *algebraic version of RGM* [56] or as a *harmonic oscillator representation of scattering equations* (HORSE) [48]. We use here a generalization of the HORSE formalism to the case of charged particle scattering proposed in Ref. [48].

Within the HORSE approach, the basis function space is split into internal and external regions. In the internal region which includes the basis states with oscillator quanta $N \leq \mathbb{N}$, the Hamiltonian completely accounts for the kinetic and potential energies. The internal region can be naturally associated with the shell-model basis space. In the external region, the Hamiltonian accounts for the relative kinetic energy of the colliding particles (and for their internal Hamiltonians if needed) only and its matrix takes a form of an infinite tridiagonal matrix of the kinetic-energy operator (plus the sum of eigenenergies of the colliding particles at the diagonal if they have an internal structure). The external region clearly represents the scattering channel under consideration. If the eigenenergies E_ν , $\nu = 0, 1, \dots$ and the respective eigenvectors of the Hamiltonian matrix in the internal region are known, one can easily calculate the S matrix, phase shifts, and other parameters characterizing the scattering process (see, e.g., Refs. [48,55,58,59]).

An interesting feature peculiar to the J -matrix method was highlighted as far back as 1974 [54]. The point is that, at the energies coinciding with the eigenvalues E_ν of the Hamiltonian matrix in the internal region, the matching condition of the J -matrix method becomes substantially simpler while the accuracy of the S -matrix and phase-shift description at these energies is much better than at the energies away from the eigenvalues E_ν [36,60,61]. Taking advantage of this feature, Yamani [61] was able to construct an analytic continuation to the complex energy plane within the R -matrix method and to obtain accurate estimates for the energies and widths of resonant states.

The single-state HORSE (SS-HORSE) method suggested in Refs. [32–34] also benefits from the improved accuracy of the HORSE approach at the eigenstates of the Hamiltonian matrix truncated to the internal region of the whole

basis space. In the case of scattering of uncharged particles interacting by a short-range potential, the phase shifts $\delta_l(E_\nu)$ in the partial wave with the orbital momentum l at the eigenenergies E_ν of the internal Hamiltonian matrix are given by [32–34]

$$\tan \delta_l(E_\nu) = -\frac{S_{\mathbb{N}+2,l}(E_\nu)}{C_{\mathbb{N}+2,l}(E_\nu)}. \quad (1)$$

Here $S_{N,l}(E)$ and $C_{N,l}(E)$ are respectively regular and irregular solutions of the free Hamiltonian at energy E in the oscillator representation for which analytical expressions can be found in Refs. [48,55,58,59]. Varying the oscillator spacing $\hbar\Omega$ and the truncation boundary \mathbb{N} of the internal oscillator basis subspace, we obtain a variation of the eigenenergy E_ν of the truncated Hamiltonian matrix over an energy interval and obtain the phase shifts $\delta_l(E)$ in that energy interval by means of Eq. (1). Next, we parametrize the phase shifts $\delta_l(E)$ as discussed in the next section to have the phase shifts and the S matrix in a wider energy interval, which makes it possible to locate the S -matrix poles.

In the case of scattering in the channels with two charged particles, following the ideas of Ref. [48], we formally cut the Coulomb interaction at the distance $r = b$. As shown in Ref. [36], an optimal value of the Coulomb cutoff distance b is the so-called *natural channel radius* b_0 [48],

$$b = b_0 \equiv r_{\mathbb{N}+2,l}^{cl} = 2r_0\sqrt{\mathbb{N}/2 + 7/4}, \quad (2)$$

i.e., b is equivalent to the classical turning point $r_{\mathbb{N}+2,l}^{cl}$ of the first oscillator function $R_{\mathbb{N}+2,l}(r)$ in the external region of the basis space. The parameter $r_0 = \sqrt{\hbar/(\mu\Omega)}$ entering Eq. (2) is the oscillator radius and μ is the reduced mass in the channel under consideration. Cutting of the Coulomb interaction at the distance $r = b_0$ does not affect the Hamiltonian matrix elements in the internal region. Therefore the shell-model Hamiltonian matrix elements in the internal region can be calculated without any modification of the Coulomb interaction between the nucleons. The scattering phase shifts δ_l^{aux} of the auxiliary Hamiltonian with the cutoff Coulomb interaction can be calculated by using the standard HORSE or SS-HORSE techniques, e.g., with the help of Eq. (1). To deduce an expression for the Coulomb-nuclear phase shifts δ_l , one should match at the distance b the plane-wave asymptotics of the auxiliary Hamiltonian wave functions with Coulomb-distorted wave function asymptotics. As a result, we get the following SS-HORSE expression for the Coulomb-nuclear phase shifts $\delta_l(E_\nu)$ at the eigenenergies E_ν of the internal Hamiltonian matrix [36]:

$$\begin{aligned} \tan \delta_l(E_\nu) &= -\frac{S_{\mathbb{N}+2,l}(E_\nu)W_b(n_l, F_l) + C_{\mathbb{N}+2,l}(E_\nu)W_b(j_l, F_l)}{S_{\mathbb{N}+2,l}(E_\nu)W_b(n_l, G_l) + C_{\mathbb{N}+2,l}(E_\nu)W_b(j_l, G_l)}. \end{aligned} \quad (3)$$

Here $j_l \equiv j_l(kr)$ and $n_l \equiv n_l(kr)$ are respectively the spherical Bessel and Neumann functions [62], while $F_l \equiv F_l(\eta, kr)$ and $G_l \equiv G_l(\eta, kr)$ are respectively the regular and irregular Coulomb functions [62]. k is the relative motion momentum, $\eta = Z_1 Z_2 e^2 \mu / (\hbar^2 k)$ is the Sommerfeld parameter, and the

quasi-Wronskian is

$$W_b(\phi, \chi) = \left(\frac{d\phi}{dr} \chi - \phi \frac{d\chi}{dr} \right) \Big|_{r=b}. \quad (4)$$

As in the case of neutral-particle scattering, we obtain the Coulomb-nuclear phase shifts $\delta_l(E)$ in some energy interval by varying the internal region boundary \mathbb{N} and the oscillator spacing $\hbar\Omega$, then parametrize the phase shifts to have them in a wider energy interval. However, the phase-shift parametrization is more complicated for channels with charged colliding particles, as discussed below.

An important scaling property of variational calculations with the harmonic-oscillator basis was revealed in Refs. [9,10]: the converging variational eigenenergies E_ν do not depend on $\hbar\Omega$ and \mathbb{N} independently but only through a scaling variable

$$s = \frac{\hbar\Omega}{\mathbb{N} + 7/2}. \quad (5)$$

This scaling property was initially proposed in Refs. [9,10] for the bound states. We have extended the scaling to the case of variational calculations with the harmonic-oscillator basis of the unbound states [32,33] within the SS-HORSE approach. The SS-HORSE extension to the case of charged particle scattering discussed here can be used to demonstrate that the long-range Coulomb interaction does not destroy the scaling property of the unbound states (see Ref. [36] for details).

B. Phase-shift parametrization

The total partial-wave scattering amplitude in the case of Coulomb and short-range interactions has the form of the sum of the purely Coulomb, $f_l^C(k)$, and Coulomb-nuclear, $f_l^{NC}(k)$, amplitudes [63],

$$f_l(k) = f_l^C(k) + f_l^{NC}(k), \quad (6)$$

which, in turn, are related to the purely Coulomb, $\sigma_l = \arg \Gamma(1 + l + i\eta)$, and Coulomb-nuclear phase shifts, δ_l , as

$$f_l^C(k) = \frac{\exp(2i\sigma_l) - 1}{2ik}, \quad (7)$$

$$f_l^{NC}(k) = \exp(2i\sigma_l) \frac{\exp(2i\delta_l) - 1}{2ik}. \quad (8)$$

Analytic properties of the Coulomb-nuclear amplitude $f_l^{NC}(k)$ in the complex momentum plane differ from the analytic properties of the scattering amplitude for neutral particles. However, the *renormalized Coulomb-nuclear amplitude* [46,47],

$$\tilde{f}_l(E) = \left[\frac{\exp(2i\delta_l) - 1}{2ik} \right] \left[\frac{\exp(2\pi\eta) - 1}{2\pi\eta} \right] c_{l\eta}, \quad (9)$$

where

$$c_{l\eta} = \prod_{n=1}^l (1 + \eta^2/n^2)^{-1} \quad (l > 0), \quad c_{0\eta} = 1 \quad (10)$$

is identical in analytic properties on the real momentum axis with the scattering amplitude for neutral particles. In

particular, the renormalized amplitude can be expressed as [46,47]

$$\tilde{f}_l(E) = \frac{k^{2l}}{\tilde{K}_l(E) - 2\eta k^{2l+1} H(\eta)(c_{l\eta})^{-1}} \quad (11)$$

in terms of the *Coulomb-modified effective-range function* [46,47]

$$\begin{aligned} \tilde{K}_l(E) &= k^{2l+1}(c_{l\eta})^{-1} \\ &\times \left\{ \frac{2\pi\eta}{\exp(2\pi\eta) - 1} [\cot \delta_l(E) - i] + 2\eta H(\eta) \right\}, \end{aligned} \quad (12)$$

where

$$H(\eta) = \Psi(i\eta) + (2i\eta)^{-1} - \ln(i\eta), \quad (13)$$

$\Psi(z)$ is the logarithmic derivative of the Γ function (digamma or Ψ function) [62], and the relative motion energy $E = \hbar^2 k^2 / (2\mu)$. In the absence of the Coulomb interaction ($\eta = 0$), the Coulomb-modified effective-range function transforms into the standard effective-range function for neutral-particle scattering,

$$\tilde{K}_l(E) = K_l(E) = k^{2l+1} \cot \delta_l, \quad (14)$$

while the renormalized amplitude becomes the conventional neutral-particle scattering amplitude,

$$f_l(E) = \frac{k^{2l}}{K_l(E) - ik^{2l+1}}. \quad (15)$$

Due to their nice analytic properties, the renormalized Coulomb-nuclear amplitude, $\tilde{f}_l(E)$, and the neutral-particle scattering amplitude, $f_l(E)$, can be used to parametrize respectively the Coulomb-nuclear and neutral-particle scattering phase shifts ensuring their correct low-energy behavior. In Refs. [35,36], we introduced an auxiliary complex-valued function embedding resonant pole parameters in the amplitude parametrization. These resonant pole parameters play the role of additional fitting parameters in the phase-shift parametrization. Here we prefer to parametrize the Coulomb-modified effective-range function (12) or the standard effective-range function for neutral-particle scattering (14) thus reducing the number of fit parameters. The resonant parameters are obtained by a numerical location of the amplitude pole as discussed below.

The Coulomb-modified effective-range function $\tilde{K}_l(E)$ as well as the effective-range function for neutral-particle scattering $K_l(E)$ is real on the real axis of momentum k , is regular in the vicinity of zero, and admits an expansion in even powers of k or, equivalently, in a power series of the relative motion energy $E = \hbar^2 k^2 / (2\mu)$ [46,47],

$$\tilde{K}_l(E) = w_0 + w_1 E + w_2 E^2 + \dots \quad (16)$$

The expansion coefficients w_0 and w_1 are related to the so-called scattering length a_l and effective range r_l [63]:

$$w_0 = -\frac{1}{a_l}, \quad w_1 = \frac{r_l \mu}{\hbar^2}. \quad (17)$$

We use the expansion coefficients w_0 , w_1 , and w_2 as fit parameters for the phase-shift parametrization. Such a parametrization works well in the case of nucleon- α scattering but may fail in other problems. Note, as seen from Eq. (12) or (14), that the positive energies at which the phase shift takes the values of $0, \pm\pi, \pm2\pi, \dots$, are the singular points of the effective-range function. In the case of possible presence of such singular points in the range of energies of interest for a particular problem, one should use a more elaborate parametrization of the effective-range function, e.g., in the form of the Padé approximant.

C. Fitting process

In the case of neutral-particle scattering, we combine Eqs. (1), (14), and (16) to obtain

$$w_0 + w_1 E + w_2 E^2 = -k^{2l+1} \frac{C_{N+2,l}(E)}{S_{N+2,l}(E)}. \quad (18)$$

In the case of charged particle scattering, we derive a more complicated equation with the help of Eq. (3) and (12):

$$\begin{aligned} w_0 + w_1 E + w_2 E^2 &= -k^{2l+1}(c_{l\eta})^{-1} \left\{ \frac{2\pi\eta}{\exp(2\pi\eta) - 1} \right. \\ &\times \left[\frac{S_{N+2,l}(E)W_b(n_l, G_l) + C_{N+2,l}(E)W_b(j_l, G_l)}{S_{N+2,l}(E)W_b(n_l, F_l) + C_{N+2,l}(E)W_b(j_l, F_l)} + i \right] \\ &\left. - 2\eta H(\eta) \right\}. \end{aligned} \quad (19)$$

Let $E_v^{(i)}$, $i = 1, 2, \dots, D$, be a set of the lowest ($\nu = 0$) or some other particular eigenvalues ($\nu > 0$) of the Hamiltonian matrix truncated to the internal region of the basis space obtained with a set of parameters $(\mathbb{N}^{(i)}, \hbar\Omega^{(i)})$, $i = 1, 2, \dots, D$. We find energies $\mathcal{E}^{(i)}$ as solutions of Eq. (18) or (19) with some trial set of the effective-range function expansion coefficients w_0 , w_1 , w_2 for each combination of parameters $(\mathbb{N}^{(i)}, \hbar\Omega^{(i)})$ [note that the oscillator basis parameter $\hbar\Omega$ enters definitions of functions $S_{N,l}(E)$ and $C_{N,l}(E)$]. The optimal set of the fit parameters w_0 , w_1 , w_2 parametrizing the phase shifts is obtained by minimizing the functional

$$\Xi = \sqrt{\frac{1}{D} \sum_{i=1}^D (E_v^{(i)} - \mathcal{E}^{(i)})^2}. \quad (20)$$

With the optimal set of the fit parameters w_0 , w_1 , w_2 we can use Eq. (18) or (19) to obtain the $\hbar\Omega$ dependencies of the eigenenergies $E_v(\hbar\Omega)$ in any basis space \mathbb{N} . Therefore, Eqs. (18) and (19) provide the extrapolation of the variational results for unbound states to larger basis spaces.

D. Resonance energy E_r and width Γ

We obtain resonance energies E_r and widths Γ by a numerical location of the S -matrix poles which coincide with the poles of the scattering amplitude. If the amplitude has a resonant pole at a complex energy $E = E_r - i\Gamma/2$, the resonance energy E_r and its width Γ are related to the real and imaginary

part of E_p [63]:

$$E_p = E_r - i \frac{\Gamma}{2}. \quad (21)$$

It follows from Eqs. (11) and (15) that locating the pole of the scattering amplitude is equivalent to solving in the complex energy plane the equation

$$\mathcal{F}(E) \equiv \tilde{K}_l(E) - 2\eta k^{2l+1} H(\eta)(c_{l\eta})^{-1} = 0 \quad (22)$$

in the case of charged particle scattering, or the equation

$$\mathcal{F}(E) \equiv K_l(E) - ik^{2l+1} = 0 \quad (23)$$

in the case of neutral particles. We can use the parametrization of functions $\tilde{K}_l(E)$ or $K_l(E)$ in Eqs. (22) and (23). To solve these equations, we calculate the integral

$$\Upsilon = \frac{1}{2\pi i} \oint_C \frac{\mathcal{F}'(E)}{\mathcal{F}(E)} dE \quad (24)$$

along some closed contour C in the complex-energy plane, where $\mathcal{F}'(E) = \frac{d\mathcal{F}}{dE}$. The contour C should surround the area where we expect to have the pole of the amplitude. According to the theory of functions of a complex variable [64], the value of Υ is equal to the number of zeros of the function $\mathcal{F}(E)$ in the area surrounded by the contour C . If needed, we modify the contour C to obtain

$$\Upsilon = 1. \quad (25)$$

The position of the pole in the energy plane is calculated as

$$E_p = \frac{1}{2\pi i} \oint_C E \frac{\mathcal{F}'(E)}{\mathcal{F}(E)} dE. \quad (26)$$

A numerical realization of the algorithm based on Eqs. (24)–(26) provides means for a fast and stable determination of the poles of scattering amplitude.

III. ELASTIC SCATTERING OF NUCLEONS BY α PARTICLE IN NCSM-SS-HORSE APPROACH

We present here an application of our SS-HORSE technique to nucleon- α scattering phase shifts and resonance parameters based on *ab initio* many-body calculations of ^5He and ^5Li nuclei within the NCSM with the realistic JISP16 and Daejeon16 NN interactions. The NCSM calculations are performed by using the code MFDn [65,66] with basis spaces including all many-body oscillator states with excitation quanta N_{\max} ranging from 2 up to 18 for both parities and with $\hbar\Omega$ values ranging from 10 to 40 MeV in steps of 2.5 MeV.

Note that, for the NCSM-SS-HORSE analysis, we need the ^5He and ^5Li energies relative respectively to the $n + \alpha$ and $p + \alpha$ thresholds. Therefore, from each of the ^5He or ^5Li NCSM odd (even) parity eigenenergies we subtract the ^4He ground-state energy obtained by the NCSM with the same $\hbar\Omega$ and the same N_{\max} (with $N_{\max} - 1$) excitation quanta, and in what follows these subtracted energies are referred to as the NCSM eigenenergies E_ν . Only these ^5He and ^5Li NCSM eigenenergies relative to the respective threshold are discussed below.

We note here that the NCSM utilizes the truncation based on the many-body oscillator quanta N_{\max} while the SS-HORSE requires the oscillator quanta truncation \mathbb{N} of the interaction describing the relative motion of nucleon and α particle. We relate \mathbb{N} to N_{\max} as

$$\mathbb{N} = N_{\max} + N_0, \quad (27)$$

where $N_0 = 1$ is the minimal oscillator quanta in our five-body $N\alpha$ systems. A justification of using this relation for the SS-HORSE analysis is obvious if the α particle is described by the simplest four-nucleon oscillator function with excitation quanta $N_{\max}^\alpha = 0$. Physically it is clear that the use of Eq. (27) for the SS-HORSE should work well also in a more general case when the α particle is presented by the wave function with $N_{\max}^\alpha > 0$ due to the dominant role of the zero-quanta component in the α particle wave function. Instead of attempting to justify algebraically the use of N_{\max} within the SS-HORSE, we suggested in Refs. [32,33] an *a posteriori* justification: we demonstrated in Refs. [32,33] that we obtained $n\alpha$ phase-shift parametrizations consistent with the NCSM results obtained with very different N_{\max} and $\hbar\Omega$ values; more, we were able to predict the NCSM results with large N_{\max} by using the phase-shift parametrizations based on the NCSM calculations with much smaller model spaces. It would clearly be impossible if the use of N_{\max} truncation for the SS-HORSE analysis did not work properly. We performed the same *a posteriori* analysis of our results in the present study of nucleon- α scattering to ensure the justification of our approach though we do not present and discuss it below. Generally, the fact that the phase shifts calculated using Eq. (1) or (3) at the NCSM eigenenergies obtained with different N_{\max} truncations form a single curve as a function of energy serves as a confirmation of the consistency of the whole NCSM-SS-HORSE approach and of the use of the NCSM N_{\max} for the SS-HORSE phase-shift calculation in particular. The ranges of N_{\max} and $\hbar\Omega$ values where this consistency is achieved differ for different NN interactions and different angular momenta and parities. Such a consistency, which can be also interpreted as a convergence of the phase-shift calculations, is seen in the figures below to be achieved in all calculations at least at largest basis spaces in some range of $\hbar\Omega$ values.

A. Phase shifts of resonant $p\alpha$ scattering

Figure 1 presents the results of the NCSM calculations of the $^5\text{Li } \frac{3}{2}^-$ ground-state energies $E_0^{(i)}$ relative to the $p + \alpha$ threshold. The respective phase shifts calculated using Eq. (3) for all ^5Li eigenstates $E_0^{(i)}$ are shown in the Fig. 2.

For the SS-HORSE analysis we should select a set of consistent (converged) NCSM eigenstates $E_0^{(i)}$ which form a single curve of the phase shifts $\delta_l(E_0^{(i)})$ vs energy, as discussed in detail in Refs. [32–36]. Alternatively one can use for the eigenstate selection the graph of $E_0^{(i)}$ vs the scaling parameter s or the graph of the Coulomb-modified effective-range function $\tilde{K}_l(E_0^{(i)})$ vs energy where the converged eigenstates should also form a single curve. Our selection of the eigenstates $E_0^{(i)}$ is illustrated by the shaded area in Fig. 1

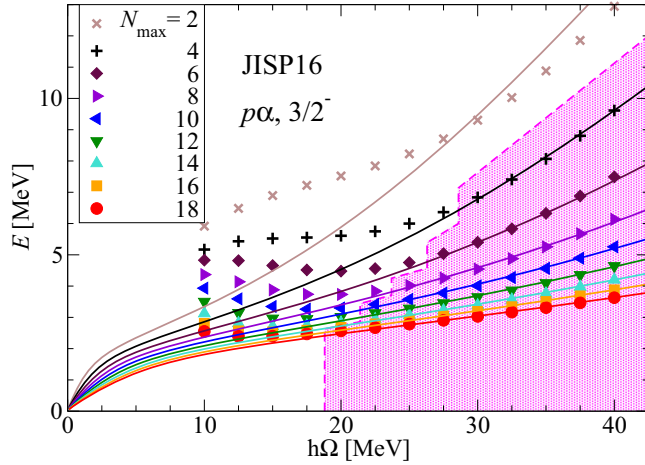


FIG. 1. The lowest ${}^5\text{Li } \frac{3}{2}^-$ eigenenergies $E_0^{(i)}$ relative to the $p + \alpha$ threshold obtained by the NCSM with the JISP16 NN interaction with various N_{max} (symbols) as functions of $\hbar\Omega$. The shaded area shows the energy values selected for the SS-HORSE analysis. Solid curves are solutions of Eq. (19) for energies E with parameters w_0 , w_1 , and w_2 obtained by the fit.

while the method of the eigenstate selection is seen from comparing Figs. 2 and 3: the symbols in Fig. 2 depict the phase shifts $\delta_1(E_0^{(i)})$ corresponding to all eigenstates $E_0^{(i)}$ while those in Fig. 3 correspond to the selected eigenstates only. More details regarding the eigenstate selection can be found in Refs. [32,33] and we will follow these established procedures without further elaboration.

A good-quality reproduction of the Coulomb-modified effective-range function points $\tilde{K}_l(E_0^{(i)})$ by the fit is illustrated in Fig. 4. We note that the quality of description of the functions $\tilde{K}_l(E)$ and $K_l(E)$ by the fit in cases of other states and interactions is approximately the same and we shall not present the graphs of these functions in what follows. A numerical estimate of the fit quality in our approach is the rms

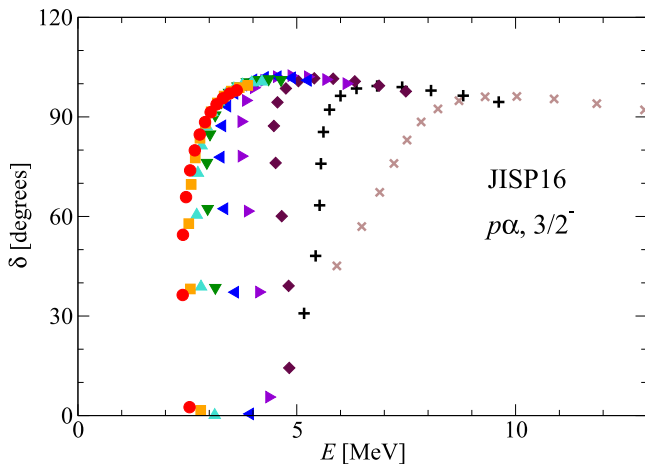


FIG. 2. $p\alpha$ scattering in the $\frac{3}{2}^-$ state with JISP16 NN interaction. The $\frac{3}{2}^- p\alpha$ phase shifts obtained directly for all calculated ${}^5\text{Li}$ eigenstates $E_0^{(i)}$ using Eq. (3) (symbols, see Fig. 1 for details).

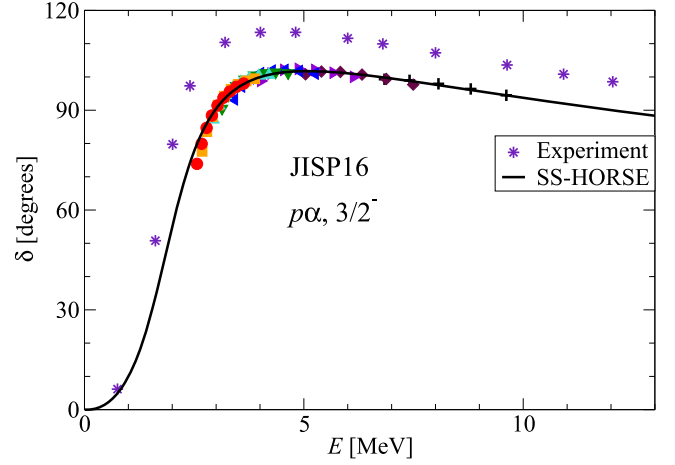


FIG. 3. $p\alpha$ scattering in the $\frac{3}{2}^-$ state with JISP16 NN interaction. The fit of the $\frac{3}{2}^- p\alpha$ phase shifts (solid curve) and the phase shifts obtained directly from the selected ${}^5\text{Li}$ eigenstates $E_0^{(i)}$ using Eq. (3) (symbols, see Fig. 1 for details) are compared. Experimental data (stars) are taken from Ref. [67].

deviation Ξ of the eigenenergies $E_0^{(i)}$ presented in Table I. It is seen that, in all cases, Ξ is of the order of few tens of keV.

Figure 3 demonstrates a good quality of the fit of the phase-shift points $\delta_1(E_0^{(i)})$. The fitted phase shifts are seen from this panel to reproduce qualitatively the results of the phase-shift analysis of the experimental data of Ref. [67]. However, the theoretical phase-shift behavior indicates that the resonance has a slightly higher energy and a larger width than observed experimentally; as a result, the theoretical phase shifts lie approximately 10 degrees below those extracted from experiment at the end of the resonance region and at higher energies.

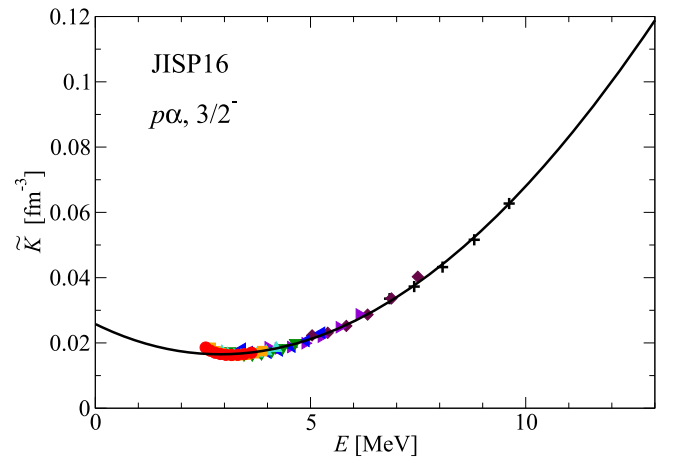


FIG. 4. Coulomb-modified effective-range function $\tilde{K}_l(E)$ for the $p\alpha$ scattering in the $\frac{3}{2}^-$ state with JISP16 NN interaction calculated by using Eq. (16) with parameters w_0 , w_1 , and w_2 obtained by the fit (solid curve) and calculated by using the right-hand side of Eq. (19) at the selected eigenenergies $E_0^{(i)}$ (symbols; see Fig. 1 for details).

TABLE I. Energies E_r and widths Γ of resonant states $\frac{3}{2}^-$ and $\frac{1}{2}^-$ in ${}^5\text{Li}$ and ${}^5\text{He}$ obtained in the NCSM-SS-HORSE approach with JISP16 and Daejeon16 NN interactions. The JISP16 results for ${}^5\text{He}$ resonances are taken from Ref. [32]. Ξ presents the rms deviation of energies obtained in the fit, D is the number of selected NCSM eigenenergies used in the fit. Δ is the spin-orbit splitting. The NCSMC results obtained with $\chi\text{EFT } NN$ and NNN interactions are from Ref. [52] and the experimental results are from Ref. [68].

	E_r (MeV)	Γ (MeV)	Ξ (keV)	D	E_r (MeV)	Γ (MeV)	Ξ (keV)	D	Δ (MeV)
${}^5\text{Li}, 3/2^-$					${}^5\text{Li}, 1/2^-$				
Expt.	1.69	1.23			3.18	6.60			1.49
JISP16	1.84	1.80	43	60	3.54	6.04	63	59	1.70
Daejeon16	1.52	1.05	24	40	3.21	5.63	50	40	1.69
NCSMC	1.77	1.70			3.11	7.90			1.34
${}^5\text{He}, 3/2^-$					${}^5\text{He}, 1/2^-$				
Expt.	0.80	0.65			2.07	5.57			1.27
JISP16 [32]	0.89	0.99	70	68	1.86	5.46	85	60	0.97
Daejeon16	0.68	0.52	22	40	2.45	5.07	48	40	1.77

The results of the calculations of the same phase shifts with the Daejeon16 NN interaction are presented in Figs. 5 and 6. It is seen that in this case we reproduce the experimental phase shifts in the resonance region even better than with JISP16. However, we can select for the SS-HORSE analysis much less NCSM results than in the case of JISP16: only the NCSM states obtained with Daejeon16 with $N_{\max} \geq 12$ are forming the same curve on the $\delta_1(E_0^{(i)})$ vs energy plot while in the JISP16 case we utilize for the SS-HORSE analysis the results with $N_{\max} \geq 4$. In other words, surprisingly, the convergence of continuum state calculations with the Daejeon16 NN interaction is slower than with JISP16 while the Daejeon16 results in a much faster convergence of NCSM calculations for bound states of light nuclei [44]. The same trends in comparing convergence of Daejeon16 and JISP16 continuum calculations are seen in all the rest results presented here.

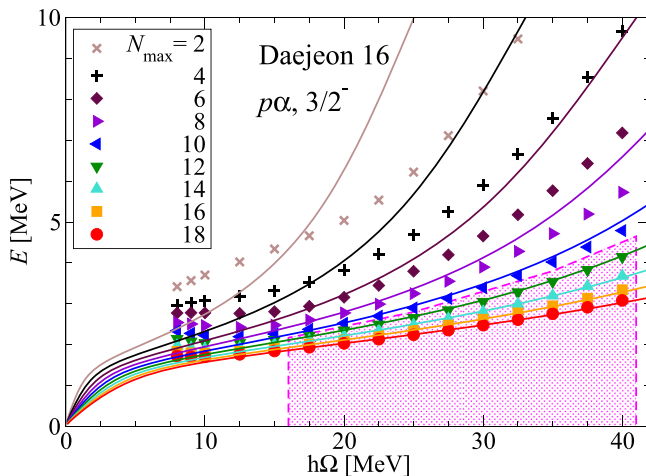


FIG. 5. The same as Fig. 1 but the lowest ${}^5\text{Li } \frac{3}{2}^-$ eigenenergies $E_0^{(i)}$ are obtained with the Daejeon16 NN interaction.

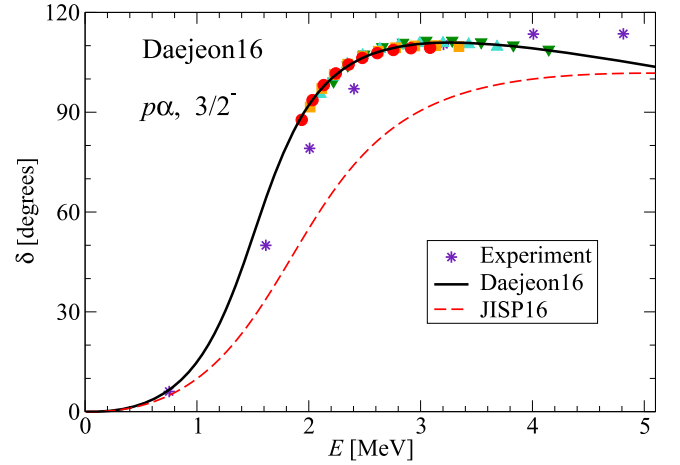


FIG. 6. $p\alpha$ scattering in the $\frac{3}{2}^-$ state with the Daejeon16 NN interaction. Dashed curve presents the phase shifts obtained with JISP16 for comparison. See Fig. 3 for other details.

The results of calculations of the $p\alpha$ scattering in the $\frac{1}{2}^-$ state with JISP16 and Daejeon16 are presented in Figs. 7–10. Both interactions reproduce well the experimental data in the resonance region while the JISP16 phase shifts are closer to the experiment at higher energies.

B. Phase shifts of resonant $n\alpha$ scattering

We have studied the $n\alpha$ scattering within the NCSM-SS-HORSE approach with the JISP16 NN interaction in Refs. [32,33]. We present for completeness here the $n\alpha$ phase shifts obtained with the Daejeon16 NN interaction. We note however that the phase shifts and resonance parameters in Refs. [32,33] were obtained by using the parametrization of the S matrix in the low-energy region while here we parametrize the effective-range function $K_I(E)$ to calculate the phase shifts and S -matrix poles associated with resonances. The effective-range function parametrization with the

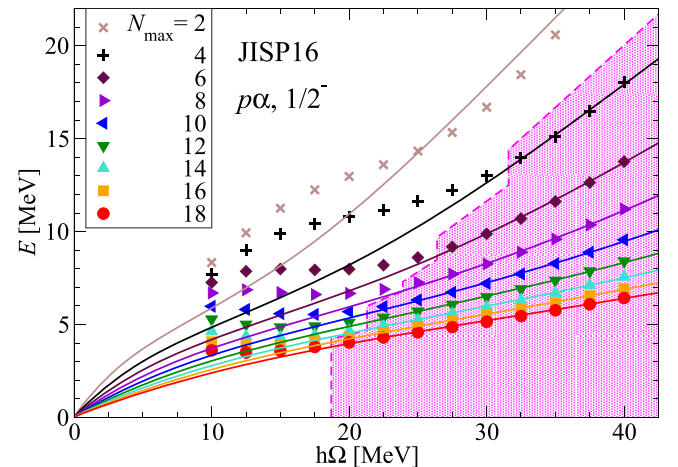


FIG. 7. The same as Fig. 1 but for the lowest ${}^5\text{Li } \frac{1}{2}^-$ eigenenergies $E_0^{(i)}$ obtained with the JISP16 NN interaction.

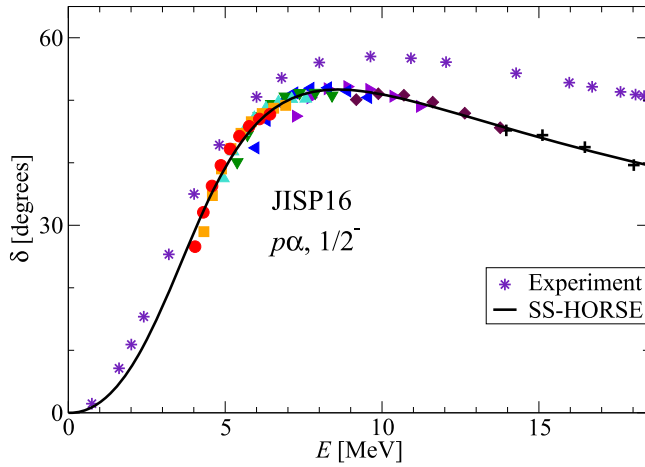


FIG. 8. $p\alpha$ scattering in the $\frac{1}{2}^-$ state with the JISP16 NN interaction. See Fig. 3 for details.

same number of parameters is more accurate in describing the phase shifts obtained directly from the NCSM eigenenergies as is seen in Fig. 11; however, this difference is pronounced in description of the wide $\frac{1}{2}^-$ resonance in ${}^5\text{He}$ only shown in Fig. 11. The difference in the phase shifts produces, of course, the difference in the energy and width of the $\frac{1}{2}^-$ resonance in ${}^5\text{He}$ while the parameters of the narrower $\frac{3}{2}^-$ resonance in ${}^5\text{He}$ are only slightly affected by the different phase-shift parametrizations.

The resonant $n\alpha$ phase shifts obtained with Daejeon16 are presented in Figs. 12–15 in comparison with those from JISP16 taken from Refs. [32,33]. As in the case of the $p\alpha$ scattering, the narrower $\frac{3}{2}^-$ resonance is better described by the Daejeon16 than by the JISP16 interaction, while the $\frac{1}{2}^-$ $n\alpha$ phase shifts are reproduced better by JISP16. We note again a faster convergence of the JISP16 calculations of $n\alpha$ scattering phase shifts as compared with those with Daejeon16.

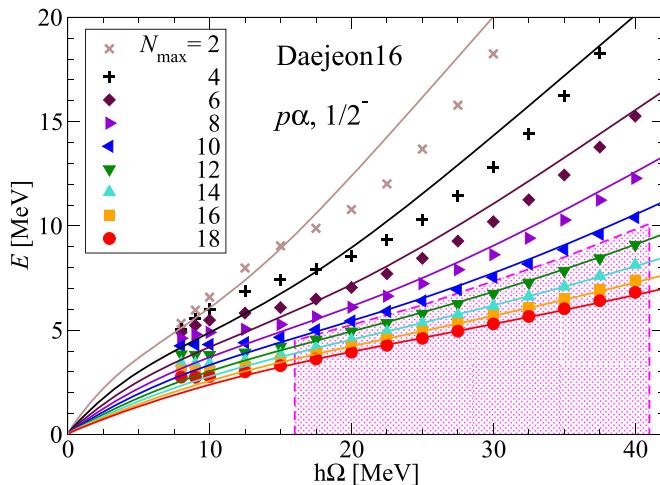


FIG. 9. The same as Fig. 1 but for the lowest ${}^5\text{Li}$ $\frac{1}{2}^-$ eigenenergies $E_0^{(i)}$ obtained with the Daejeon16 NN interaction.

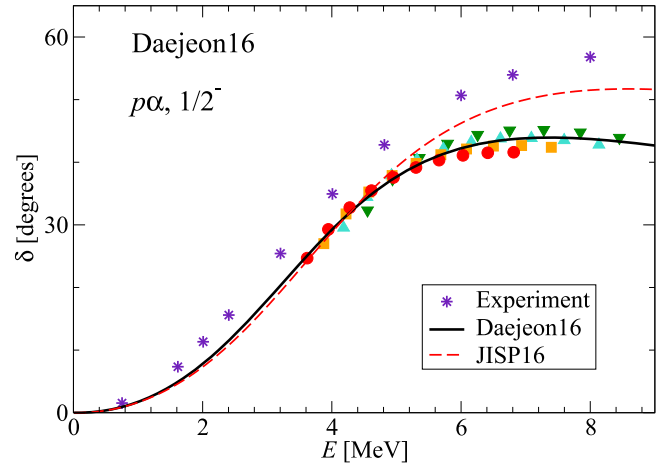


FIG. 10. $p\alpha$ scattering in the $\frac{1}{2}^-$ state with the Daejeon16 NN interaction in comparison with that obtained with JISP16. See Fig. 3 for details.

C. $\frac{3}{2}^-$ and $\frac{1}{2}^-$ resonances in ${}^5\text{Li}$ and ${}^5\text{He}$ nuclei

The results for energies and widths of the $\frac{3}{2}^-$ and $\frac{1}{2}^-$ resonances in ${}^5\text{Li}$ and ${}^5\text{He}$ nuclei with respect to the nucleon + α threshold obtained by the numerical location of the scattering amplitude poles, as described in Sec. II D, are presented in Table I. For comparison, we present in Table I also the results for the ${}^5\text{Li}$ resonances obtained with χEFT NN and NNN interactions in the *ab initio* NCSM/RGM approach in Ref. [52]. We note that the energy of the resonance was calculated in Ref. [52] as a position of the maximum of the derivative $\frac{d\delta_l(E)}{dE}$ while the resonance width was evaluated as $\Gamma = 2/(d\delta_l/dE)|_{E=E_r}$. The phase shift $\delta_l(E)$ may have a contribution from a nonresonant background which can result in some shift of the resonance energy E_r and in a modification

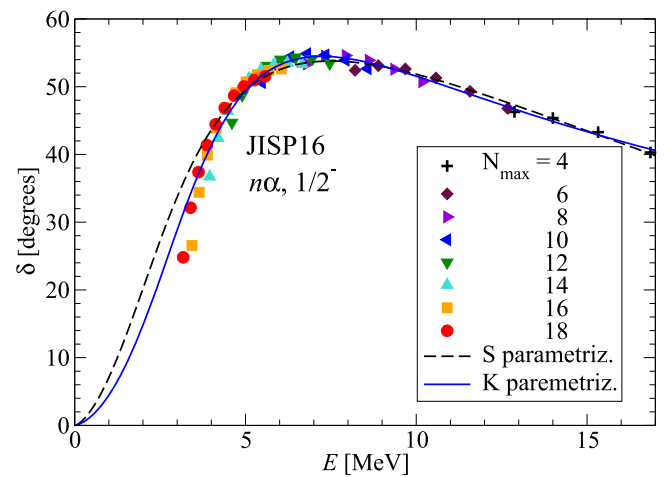


FIG. 11. The fit of the JISP16 $\frac{1}{2}^-$ $n\alpha$ phase shifts obtained directly from the selected ${}^5\text{He}$ eigenstates $E_0^{(i)}$ using Eq. (3) (symbols, see Fig. 1 for details) using the S -matrix parametrization [32] (dashed curve) and parametrization of the effective-range function $K_l(E)$ (solid curve).

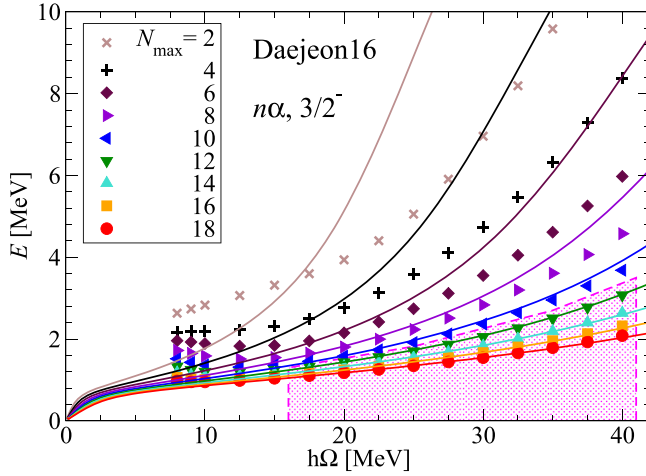


FIG. 12. The same as Fig. 1 but for the lowest ${}^5\text{He } \frac{3}{2}^-$ eigenenergies $E_0^{(i)}$ obtained with the Daejeon16 NN interaction.

of its width Γ in such calculations as compared with a more theoretically substantiated method relating the resonance parameters to the S -matrix and/or scattering-amplitude pole. The differences in energy and width from these different theoretical approaches may be large for wide resonances.

We note that all *ab initio* calculations of resonance parameters in ${}^5\text{Li}$ and ${}^5\text{He}$ nuclei provide a good description of the experimental data of Ref. [68]. The difference in $\frac{3}{2}^-$ resonance energies in both nuclei obtained with different interactions is less than 300 keV, and the experimental resonance energies are within the respective intervals of predictions obtained with different interactions. The theoretical predictions for the $\frac{3}{2}^-$ resonance widths also embrace the experimental values. However, the spread of theoretical predictions for the $\frac{3}{2}^-$ resonance width is about 750 keV in the case of ${}^5\text{Li}$ and about 500 keV in the case of ${}^5\text{He}$ that appear relatively large compared with the widths.

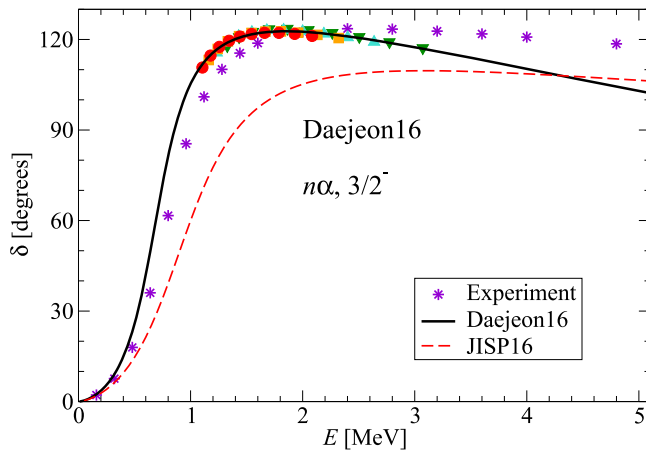


FIG. 13. $n\alpha$ scattering in the $\frac{3}{2}^-$ states with the Daejeon16 NN interaction in comparison with that obtained with JISP16 in Ref. [32]. Experimental data (stars) are taken from Ref. [69]. See Fig. 3 for other details.

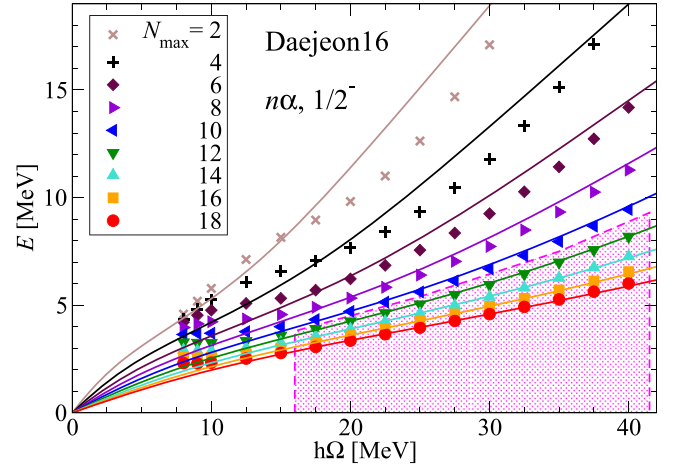


FIG. 14. The same as Fig. 1 but for the lowest ${}^5\text{He } \frac{1}{2}^-$ eigenenergies $E_0^{(i)}$ obtained with the Daejeon16 NN interaction.

In the case of the wider $\frac{1}{2}^-$ resonances in ${}^5\text{Li}$ and ${}^5\text{He}$ nuclei, the spreads of predictions for ${}^5\text{Li}$ also embrace the respective experimental energy and width values while our predictions for the ${}^5\text{He}$ resonance energy are slightly above and, for the width, are slightly below the experiment. However, the spreads of the theoretical predictions for both energy and width of the $\frac{1}{2}^-$ resonances in ${}^5\text{Li}$ and ${}^5\text{He}$ do not exceed approximately 600 keV with the exception of the NCSM/RGM $\chi\text{EFT } NN + NNN$ prediction for the $\frac{1}{2}^-$ ${}^5\text{Li}$ resonance width. Nevertheless, even the 2.3 MeV difference between our Daejeon16 and the $\chi\text{EFT } NN + NNN$ prediction of Ref. [52] for the $\frac{1}{2}^-$ ${}^5\text{Li}$ resonance width is much smaller than the experimental width. Therefore, we can say that the relative accuracy of the *ab initio* predictions for the $\frac{1}{2}^-$ resonances in ${}^5\text{Li}$ and ${}^5\text{He}$ nuclei is much better than that for the $\frac{3}{2}^-$ resonances.

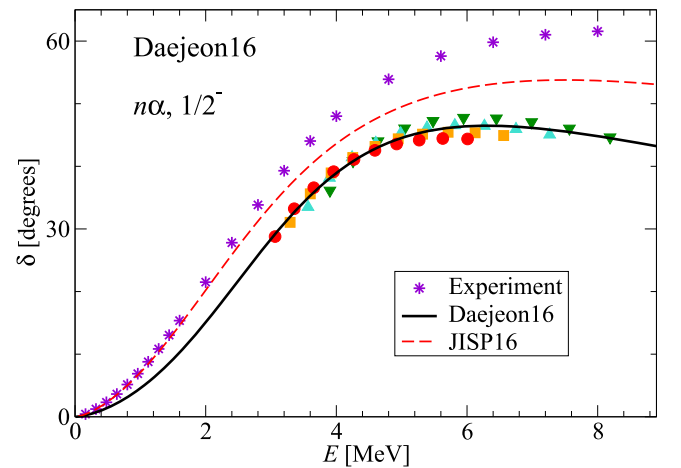


FIG. 15. $n\alpha$ scattering in the $\frac{1}{2}^-$ states with the Daejeon16 NN interaction in comparison with that obtained with JISP16 in Ref. [32]. Experimental data (stars) are taken from Ref. [69]. See Fig. 3 for other details.

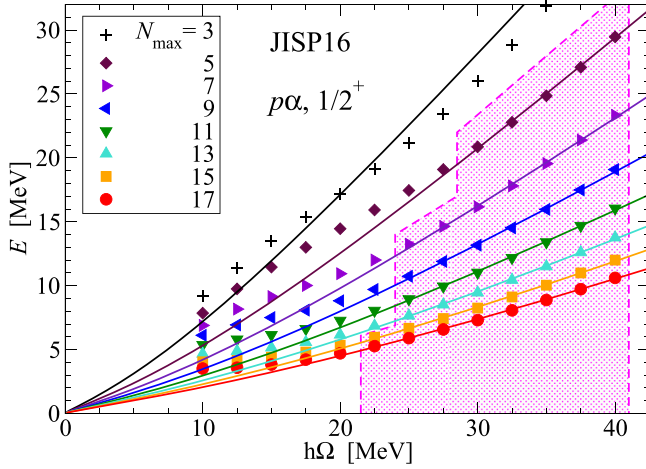


FIG. 16. The same as Fig. 1 but for the lowest ${}^5\text{Li } \frac{1}{2}^+$ eigenenergies $E_0^{(i)}$ obtained with the JISP16 NN interaction.

The difference $\Delta = (E_r^{1/2^-} - E_r^{3/2^-})$ between the energies of the $\frac{1}{2}^-$ and $\frac{3}{2}^-$ resonances in ${}^5\text{He}$ and ${}^5\text{Li}$ nuclei is conventionally associated with the spin-orbit splitting of neutrons and protons, respectively, in the p shell. We note however that this interpretation should be taken with care of since the energy difference Δ has additional contributions from the central part of the n - α interaction potential and from the kinetic energy of the relative motion of nucleon and α particle [70]. The Δ values are presented in Table I. The χ EFT $NN + NNN$ interaction slightly underestimates the proton spin-orbit splitting; Daejeon16 overestimates both proton and neutron spin-orbit splittings while JISP16 overestimates the proton and underestimates the neutron spin-orbit splitting. It is interesting to note that the differences between our predictions with JISP16 and Daejeon16 for the ${}^5\text{Li}$ resonance energies are of the order of 300 keV while the difference in the respective proton spin-orbit splittings Δ is only about 75 keV. It is more important to note that both JISP16 and Daejeon16 NN interactions are

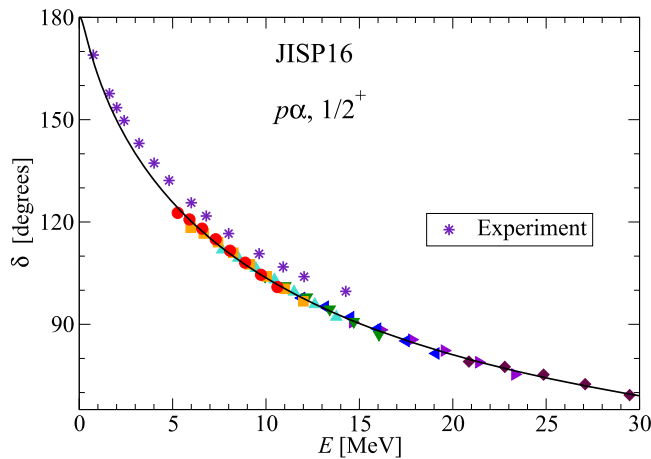


FIG. 17. Nonresonant $p\alpha$ scattering in the $\frac{1}{2}^+$ state with the JISP16 NN interaction. See Fig. 3 for details and Fig. 16 for the correspondence of the symbols to the NCSM calculations with various N_{max} values.

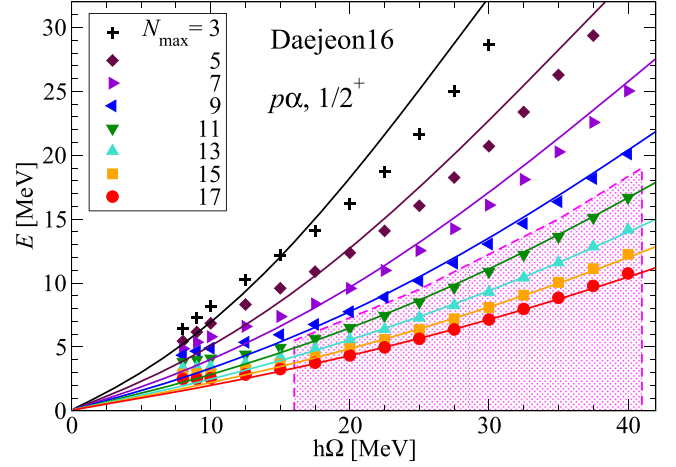


FIG. 18. The same as Fig. 1 but for the lowest ${}^5\text{Li } \frac{1}{2}^+$ eigenenergies $E_0^{(i)}$ obtained with the Daejeon16 NN interaction.

charge independent; however the Daejeon16 supports nearly the same p -shell spin-orbit splittings for protons and neutrons while the JISP16 suggests a large difference of about 800 keV between the proton and neutron p -shell spin-orbit splittings which significantly exceeds the experimental value for this difference of approximately 200 keV.

D. Nonresonant $p\alpha$ scattering

We have used the NCSM-SS-HORSE approach in Ref. [32–34] for calculations of resonant as well as nonresonant $p\alpha$ scattering. The nonresonant phase shifts can be also calculated within the current extension of the NCSM-SS-HORSE to the case of channels with charged colliding particles. Contrary to the phase-shift parametrizations based on the S -matrix analytic properties utilized in Refs. [32–34], we use the same Coulomb-modified effective-range function parametrization of Eq. (16) for both resonant and nonresonant scattering.

The results of calculations of the nonresonant $p\alpha$ scattering phase shifts in the $\frac{1}{2}^+$ state with JISP16 and Daejeon16 NN interactions are presented in Figs. 16–19. It is seen that JISP16 provides a faster convergence of the phase shifts in this case, too. The results obtained with JISP16 and Daejeon16 are close to each other and reproduce well the experimental phase shifts of Ref. [67].

E. Nonresonant $n\alpha$ scattering

For completeness, we present here the results of calculations of the nonresonant $\frac{1}{2}^+ n\alpha$ scattering phase shifts with the Daejeon16 NN interaction. The results of the NCSM calculations of the lowest $\frac{1}{2}^+ {}^5\text{He}$ states with Daejeon16 and the selection of eigenstates for the SS-HORSE analysis is shown in Fig. 20; the obtained $\frac{1}{2}^+ n\alpha$ phase shifts are presented in Fig. 21 in comparison with the respective JISP16 phase shifts from Ref. [32] and the results of the phase-shift analysis of Ref. [69]. As in the case of the nonresonant $p\alpha$ scattering, the $\frac{1}{2}^+ n\alpha$ phase shifts obtained with JISP16 and Daejeon16

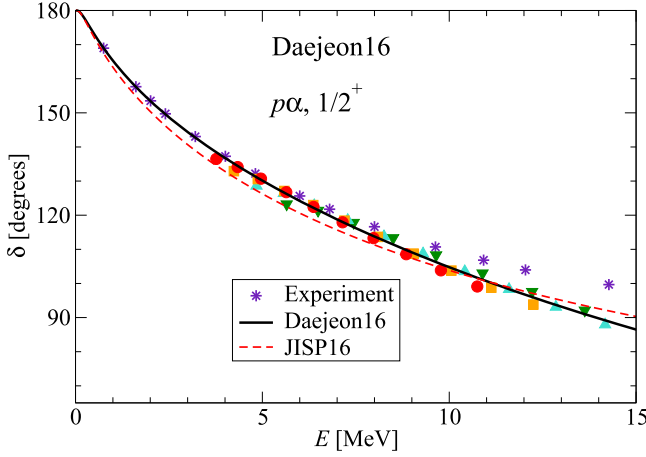


FIG. 19. Nonresonant $p\alpha$ scattering in the $\frac{1}{2}^+$ state with the Daejeon16 NN interaction in comparison with that obtained with JISP16. See Fig. 3 for details and Fig. 18 for the correspondence of the symbols to the NCSM calculations with various N_{\max} values.

NN interactions are close to each other and reproduce well the experimental phase shifts of Ref. [69].

IV. SUMMARY

We present here an extension of the *ab initio* NCSM-SS-HORSE approach to the case of channels with charged colliding particles where the relative motion wave-function asymptotics is distorted by the Coulomb interaction. The extended approach is applied to the study of $p\alpha$ scattering and resonances in the ^5Li nucleus with realistic JISP16 and Daejeon16 NN interactions. The analysis of the $n\alpha$ scattering and resonances in the ^5He nucleus with the JISP16 NN interaction has been performed by us in Refs. [32–34]; we complete this analysis here by the corresponding calculations with Daejeon16.

We demonstrate that the extended NCSM-SS-HORSE approach works with approximately the same accuracy and

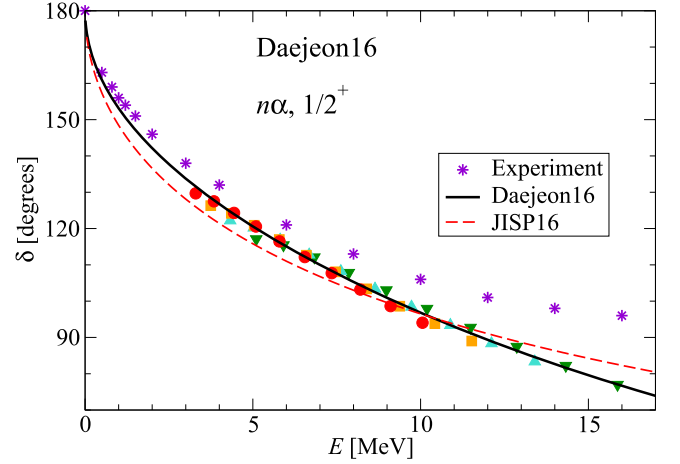


FIG. 21. Nonresonant $n\alpha$ scattering in the $\frac{1}{2}^+$ state with the Daejeon16 NN interaction in comparison with that obtained with JISP16 in Ref. [32]. Experimental data (stars) are taken from Ref. [69]. See Fig. 3 for other details and Fig. 20 for the correspondence of the symbols to the NCSM calculations with various N_{\max} values.

convergence rate as its nonextended version applicable to the channels with neutral particles. Surprisingly, we obtain that the JISP16 interaction provides a faster convergence of the $n\alpha$ and $p\alpha$ phase shifts than the Daejeon16 while the convergence of bound-state energies in light nuclei within NCSM is much faster with Daejeon16 than with JISP16 [44].

Both JISP16 and Daejeon16 provide a good description of the $\frac{3}{2}^-$ and $\frac{1}{2}^-$ resonances in ^5Li and ^5He nuclei as well as of the $\frac{1}{2}^+$ nonresonant $n\alpha$ and $p\alpha$ phase shifts. However, the spin-orbit splitting of nucleons in the p shell is overestimated by the charge-independent Daejeon16 NN interaction which supports nearly the same spin-orbit splittings for neutrons and protons; the JISP16 NN interaction, which is also charge independent, overestimates the p -shell spin-orbit splitting for protons and underestimates the p -shell spin-orbit splitting for neutrons.

ACKNOWLEDGMENTS

We are thankful to V. D. Efros and P. Maris for valuable discussions. This work was supported in part by the U.S. Department of Energy under Grants No. DESC00018223 (SciDAC/NUCLEI) and No. DE-FG02-87ER40371, and by the Rare Isotope Science Project of Institute for Basic Science funded by Ministry of Science and ICT and National Research Foundation of Korea (2013M7A1A1075764). The development and application of the SS-HORSE approach is supported by the Russian Science Foundation under Grant No. 16-12-10048. Computational resources were provided by the National Energy Research Scientific Computing Center (NERSC), which is supported by the Office of Science of the U.S. Department of Energy under Contract No. DE-AC02-05CH11231, and by the Supercomputing Center/Korea Institute of Science and Technology Information including technical support (KSC-2015-C3-003).

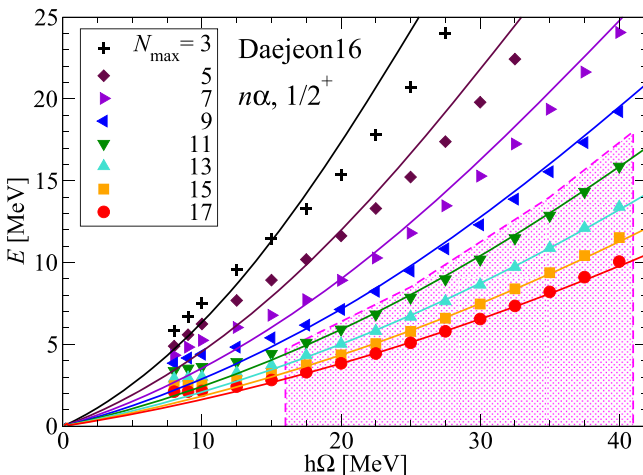


FIG. 20. The same as Fig. 1 but for the lowest ^5He $\frac{1}{2}^+$ eigenenergies $E_0^{(i)}$ obtained with the Daejeon16 NN interaction.

- [1] W. Leidemann and G. Orlandini, *Prog. Part. Nucl. Phys.* **68**, 158 (2013).
- [2] S. C. Pieper and R. B. Wiringa, *Annu. Rev. Nucl. Part. Sci.* **51**, 53 (2001).
- [3] B. R. Barrett, P. Navrátil, and J. P. Vary, *Prog. Part. Nucl. Phys.* **69**, 131 (2013).
- [4] H. Kümmela, K. H. Lührmann, and J. Zabolitzky, *Phys. Rep.* **36**, 1 (1978).
- [5] G. Hagen, D. J. Dean, M. Hjorth-Jensen, T. Papenbrock, and A. Schwenk, *Phys. Rev. C* **76**, 044305 (2007).
- [6] D. Lee, *Prog. Part. Nucl. Phys.* **63**, 117 (2009).
- [7] E. Epelbaum, H. Krebs, D. Lee, and Ulf-G. Meißner, *Phys. Rev. Lett.* **106**, 192501 (2011).
- [8] P. Maris, J. P. Vary, and A. M. Shirokov, *Phys. Rev. C* **79**, 014308 (2009).
- [9] S. A. Coon, M. I. Avetian, M. K. G. Kruse, U. van Kolck, P. Maris, and J. P. Vary, *Phys. Rev. C* **86**, 054002 (2012).
- [10] S. A. Coon, in *Proceedings - International Workshop Nuclear Theory in the Supercomputing Era (NTSE-2012)*, Khabarovsk, Russia, June 18–22, 2012, edited by A. M. Shirokov and A. I. Mazur (Pacific National University, Khabarovsk, 2013), p. 171; http://www.ntse-2012.khb.ru/Proc/S_Coon.pdf.
- [11] R. J. Furnstahl, G. Hagen, and T. Papenbrock, *Phys. Rev. C* **86**, 031301(R) (2012).
- [12] S. N. More, A. Ekstrom, R. J. Furnstahl, G. Hagen, and T. Papenbrock, *Phys. Rev. C* **87**, 044326 (2013).
- [13] M. K. G. Kruse, E. D. Jurgenson, P. Navrátil, B. R. Barrett, and W. E. Ormand, *Phys. Rev. C* **87**, 044301 (2013).
- [14] D. Sääf and C. Forssén, *Phys. Rev. C* **89**, 011303 (2014).
- [15] R. J. Furnstahl, S. N. More, and T. Papenbrock, *Phys. Rev. C* **89**, 044301 (2014).
- [16] S. König, S. K. Bogner, R. J. Furnstahl, S. N. More, and T. Papenbrock, *Phys. Rev. C* **90**, 064007 (2014).
- [17] R. J. Furnstahl, G. Hagen, T. Papenbrock, and K. A. Wendt, *J. Phys. G* **42**, 034032 (2015).
- [18] K. A. Wendt, C. Forssén, T. Papenbrock, and D. Sääf, *Phys. Rev. C* **91**, 061301 (2015).
- [19] S. A. Coon and M. K. G. Kruse, *Int. J. Mod. Phys. E* **25**, 1641011 (2016).
- [20] I. J. Shin, Y. Kim, P. Maris, J. P. Vary, C. Forssén, J. Rotureau, and N. Michel, *J. Phys. G* **44**, 075103 (2017).
- [21] A. Negoita, G. R. Luecke, J. P. Vary, P. Maris, A. M. Shirokov, I. J. Shin, Y. Kim, E. G. Ng, and C. Yang, in *Proceedings of the 9th International Conference on Computational Logics, Algebras, Programming, Tools, and Benchmarking (COMPUTATION TOOLS 2018)*, February 18–22, 2018, Barcelona, Spain (IARIA, 2018), p. 20; [arXiv:1803.03215](https://arxiv.org/abs/1803.03215) [physics.comp-ph] (2018).
- [22] L. D. Faddeev and S. P. Merkuriev, *Quantum Scattering Theory for Several Particle Systems* (Kluwer, Dordrecht, 1993).
- [23] E. O. Alt, P. Grassberger, and W. Sandhas, *Nucl. Phys. B* **2**, 167 (1967).
- [24] P. Navrátil, R. Roth, and S. Quaglioni, *Phys. Rev. C* **82**, 034609 (2010).
- [25] P. Navrátil, S. Quaglioni, I. Stetcu, and B. R. Barrett, *J. Phys. G* **36**, 083101 (2009).
- [26] P. Navrátil, S. Quaglioni, G. Hupin, C. Romero-Redondo, and A. Calci, *Phys. Scr.* **91**, 053002 (2016).
- [27] V. D. Efros, W. Leidemann, G. Orlandini, and N. Barnea, *J. Phys. G* **34**, R459 (2007).
- [28] K. M. Nollett, S. C. Pieper, R. B. Wiringa, J. Carlson, and G. M. Hale, *Phys. Rev. Lett.* **99**, 022502 (2007).
- [29] G. Papadimitriou, J. Rotureau, N. Michel, M. Płoszajczak, and B. R. Barrett, *Phys. Rev. C* **88**, 044318 (2013).
- [30] A. M. Shirokov, A. I. Mazur, J. P. Vary, and E. A. Mazur, *Phys. Rev. C* **79**, 014610 (2009).
- [31] A. M. Shirokov, A. I. Mazur, E. A. Mazur, and J. P. Vary, *Appl. Math. Inf. Sci.* **3**, 245 (2009).
- [32] A. M. Shirokov, A. I. Mazur, I. A. Mazur, and J. P. Vary, *Phys. Rev. C* **94**, 064320 (2016).
- [33] A. I. Mazur, A. M. Shirokov, I. A. Mazur, and J. P. Vary, in *Proceedings - International Conference Nuclear Theory in the Supercomputing Era (NTSE-2014)*, Khabarovsk, Russia, June 23–27, 2014, edited by A. M. Shirokov and A. I. Mazur (Pacific National University, Khabarovsk, 2016), p. 183; <http://www.ntse-2014.khb.ru/Proc/A.Mazur.pdf>.
- [34] I. A. Mazur, A. M. Shirokov, A. I. Mazur, and J. P. Vary, *Phys. Part. Nucl.* **48**, 84 (2017).
- [35] L. D. Blokhintsev, A. I. Mazur, I. A. Mazur, D. A. Savin, and A. M. Shirokov, *Yad. Fiz.* **80**, 102 (2017) [*Phys. Atom. Nucl.* **80**, 226 (2017)].
- [36] L. D. Blokhintsev, A. I. Mazur, I. A. Mazur, D. A. Savin, and A. M. Shirokov, *Yad. Fiz.* **80**, 619 (2017) [*Phys. Atom. Nucl.* **80**, 1093 (2017)].
- [37] A. M. Shirokov, J. P. Vary, A. I. Mazur, and T. A. Weber, *Phys. Lett. B* **644**, 33 (2007) (a Fortran code generating the JISP16 matrix elements is available at http://lib.dr.iastate.edu/energy_datasets/2/).
- [38] R. I. Jibuti and N. B. Krupennikova, *The Method of Hyper-spherical Functions in the Quantum Mechanics of Few Bodies* (Metsniereba, Tbilisi, 1984) (in Russian).
- [39] R. I. Jibuti, *Fiz. Elem. Chastits At. Yadra* **14**, 741 (1983).
- [40] A. M. Shirokov, G. Papadimitriou, A. I. Mazur, I. A. Mazur, R. Roth, and J. P. Vary, in *Proceedings - International Conference Nuclear Theory in the Supercomputing Era (NTSE-2014)*, Khabarovsk, Russia, June 23–27, 2014, edited by A. M. Shirokov and A. I. Mazur (Pacific National University, Khabarovsk, 2016), p. 174; <http://www.ntse-2014.khb.ru/Proc/Shirokov.pdf>.
- [41] A. M. Shirokov, G. Papadimitriou, A. I. Mazur, I. A. Mazur, R. Roth, and J. P. Vary, *Phys. Rev. Lett.* **117**, 182502 (2016).
- [42] I. A. Mazur, A. M. Shirokov, A. I. Mazur, I. J. Shin, Y. Kim, and J. P. Vary, in *Proceedings - International Conference Nuclear Theory in the Supercomputing Era (NTSE-2016)*, Khabarovsk, Russia, September 19–23, 2016, edited by A. M. Shirokov and A. I. Mazur (Pacific National University, Khabarovsk, Russia, 2018), p. 280; <http://www.ntse-2016.khb.ru/Proc/IMazur.pdf>.
- [43] K. Kisamori *et al.*, *Phys. Rev. Lett.* **116**, 052501 (2016).
- [44] A. M. Shirokov, I. J. Shin, Y. Kim, M. Sosonkina, P. Maris, and J. P. Vary, *Phys. Lett. B* **761**, 87 (2016) (a Fortran code generating the Daejeon16 matrix elements is available at http://lib.dr.iastate.edu/energy_datasets/1/).
- [45] D. R. Entem and R. Machleidt, *Phys. Lett. B* **524**, 93 (2002); *Phys. Rev. C* **68**, 041001(R) (2003).
- [46] J. Hamilton, I. Överbö, and B. Tromborg, *Nucl. Phys. B* **60**, 443 (1973).
- [47] H. van Haeringen, *Charged-Particle Interactions. Theory and Formulas* (Coulomb Press Leyden, Leiden, 1985).
- [48] J. M. Bang, A. I. Mazur, A. M. Shirokov, Yu. F. Smirnov, and S. A. Zaytsev, *Ann. Phys. (NY)* **280**, 299 (2000).

- [49] G. Hagen, D. J. Dean, M. Hjorth-Jensen, and T. Papenbrock, *Phys. Lett. B* **656**, 169 (2007).
- [50] S. Quaglioni and P. Navrátil, *Phys. Rev. C* **79**, 044606 (2009).
- [51] G. Hupin, J. Langhammer, P. Navrátil, S. Quaglioni, A. Calci, and R. Roth, *Phys. Rev. C* **88**, 054622 (2013).
- [52] G. Hupin, S. Quaglioni, and P. Navrátil, *Phys. Rev. C* **90**, 061601(R) (2014).
- [53] R. Lazauskas, *Phys. Rev. C* **97**, 044002 (2018).
- [54] E. J. Heller and H. A. Yamani, *Phys. Rev. A* **9**, 1201 (1974).
- [55] H. A. Yamani and L. J. Fishman, *J. Math. Phys.* **16**, 410 (1975).
- [56] G. F. Filippov and I. P. Okhrimenko, *Yad. Fiz.* **32**, 932 (1980) [*Sov. J. Nucl. Phys.* **32**, 480 (1980)]; G. F. Filippov, *Yad. Fiz.* **33**, 928 (1981) [*Sov. J. Nucl. Phys.* **33**, 488 (1981)].
- [57] Yu. F. Smirnov and Yu. I. Nechaev, *Kinam* **4**, 445 (1982); Yu. I. Nechaev and Yu. F. Smirnov, *Yad. Fiz.* **35**, 1385 (1982) [*Sov. J. Nucl. Phys.* **35**, 808 (1982)].
- [58] A. M. Shirokov, Yu. F. Smirnov, and S. A. Zaytsev, in *Modern Problems in Quantum Theory*, edited by V. I. Savrin and O. A. Khrustalev (Moscow State University, Moscow, 1998), p. 184.
- [59] S. A. Zaytsev, Yu. F. Smirnov, and A. M. Shirokov, *Teor. Mat. Fiz.* **117**, 227 (1998) [*Theor. Math. Phys.* **117**, 1291 (1998)].
- [60] H. A. Yamani and M. S. Abdelmonem, *J. Phys. A: Math. Gen.* **26**, L1183 (1993).
- [61] H. A. Yamani, *Eur. J. Phys.* **34**, 1025 (2013).
- [62] *Handbook of Mathematical Functions*, edited by M. Abramowitz and I. A. Stegun (Dover, New York, 1972); NIST digital library of mathematical functions, <http://dlmf.nist.gov/>.
- [63] R. G. Newton, *Scattering Theory of Waves and Particles*, 2nd ed. (Springer-Verlag, New York, 1982).
- [64] A. G. Sveshnikov and A. N. Tikhonov, *The Theory of Functions of a Complex Variable*, 2nd ed. (Mir Publishers, Moscow, 1978).
- [65] P. Maris, M. Sosonkina, J. P. Vary, E. G. Ng, and C. Yang, *Procedia Comput. Sci.* **1**, 97 (2010).
- [66] H. M. Aktulga, C. Yang, E. G. Ng, P. Maris, and J. P. Vary, *Concurr. Comput.: Pract. Exp.* **26**, 2631 (2014).
- [67] D. C. Dodder, G. M. Hale, N. Jarmie, J. H. Jett, P. W. Keaton, Jr., R. A. Nisley, and K. Witte, *Phys. Rev. C* **15**, 518 (1977).
- [68] A. Csótó and G. M. Hale, *Phys. Rev. C* **55**, 536 (1997).
- [69] R. A. Arndt, D. D. Long, and L. D. Roper, *Nucl. Phys. A* **209**, 429 (1973).
- [70] S. Aoyama, *Phys. Rev. C* **59**, 531 (1999).